

## EFFECTIVE LINK TRIGGERS TO IMPROVE HANDOVER PERFORMANCE

S. Woon N. Golmie Y. A. Şekercioğlu\*  
 National Institute of Standards and Technology  
 Gaithersburg, Maryland, USA

## ABSTRACT

Effective link layer triggering is the key in order to enable fast and reliable handovers across different access networks. In this paper, we investigate the use of signal strength as part of the trigger mechanism. We propose an analytical model to estimate the anticipation required in order to achieve a target handover packet loss performance, for both voice and video traffic patterns. Numerical results from the analytical model are presented and compared to simulation data obtained for realistic handover scenarios.

## I. INTRODUCTION

The rapidly expanding field of mobile communications over the last decade has spawned a number of different wireless communication systems. This includes IEEE 802.11, IEEE 802.16, UMTS, and Bluetooth, just to name a few. Such a variety of wireless access systems results in heterogeneous networks that can offer multiple overlapping coverage with different technologies [11, 5]. An area of interest is the development of Mobile Stations (MSs) equipped with multiple interfaces to handle different technologies [3, 7]. Handovers from one interface to another typically involve the execution of a combination of layer 2 and layer 3 handovers. These handovers may be lengthy [8, 6] and hence disruptive to the MS's communications. This is unacceptable for time-sensitive and real time applications, such as voice or video.

In this paper, the handover performance of switching between interfaces and its impact on real time applications are investigated. We use the link going down trigger to improve the handover performance, and propose methods to set appropriate thresholds for this trigger. More specifically, we first evaluate our approach using an ideal path loss model and constant traffic patterns. An expression is derived to calculate the required link going down signal threshold for a specified handover packet loss at various MS speeds. Extending the path loss model to cover more realistic operating environments where signal fluctuations are observed, as for example in the case of shadowing, we investigate weighted averaging to stabilize signal strength readings and interpolation to maintain a correlation between the trigger threshold and the MS speed. We show that these methods can be effectively used to calculate the threshold required to minimize handover packet loss, for both constant and bursty traffic.

The remainder of this article is structured as follows. In section II, we describe the link layer triggers used for handovers. In section III, we present an analytical model for setting the link going down threshold. Section IV presents numerical results to

evaluate the model. Finally, Section V offers concluding remarks.

## II. USING LINK LAYER TRIGGERS FOR HANDOVERS

Handovers generally occur when a MS moves away from its current cell coverage. When the signal level or error rate becomes unacceptable, the handover is performed where the MS connects to another point of access. Link triggers can be used within the Internet Architecture to provide performance benefits as presented in [2]. In the case where multiple interfaces are available on the MS, the 802.21 Media Independent Handover (MIH) [1] framework currently being developed can be used to facilitate both vertical and horizontal handover. The framework defines triggers which are used between layers to communicate specific events.

As mentioned earlier, the main motivation of this study is to minimize the packet lost while a handover is performed. The Link Going Down (LGD) trigger from the MIH framework can be used to achieve this. In this study, it is triggered when the received signal level is below the LGD power level threshold  $P_{l_{gd}}$  that normally has a higher value than the receive power level threshold  $P_{rx_{thresh}}$ . Without LGD, the mobility manager residing on the MS and in charge of the decision to switch interfaces will not begin to configure the connection on the new interface until the current connection is lost. This interrupts the traffic flow for the whole duration of the layer 2 and layer 3 handover, as illustrated in Fig. 1a. The LGD trigger allows the mobility manager to be informed in advance about the imminent loss of connection over the current interface. It is then able to configure the connection on a new interface before the disconnection takes place as seen in Fig. 1b. The required anticipation can be achieved by adjusting the difference between  $P_{rx_{thresh}}$  and  $P_{l_{gd}}$  appropriately as follows:

$$P_{l_{gd}} = \alpha P_{rx_{thresh}} \quad \alpha \geq 1 \quad (1)$$

where  $\alpha$  is the power level threshold coefficient. In this equation,  $\alpha$  is the key component being studied to determine a suitable value for a minimal handover packet loss. The speed of the MS also needs to be considered as part of the anticipation, since it affects the time it takes the signal to vary from  $P_{l_{gd}}$  to  $P_{rx_{thresh}}$ .

## III. SETTING LINK TRIGGER THRESHOLD

In this section we propose an analytical method for effectively setting  $P_{l_{gd}}$ . Given a path loss model, our analysis relates the ratio of time during a handover,  $R_{time}$ , the MS is disconnected, to  $\alpha$ , and the speed of the MS,  $v$ . Observe that a suitable path loss model that accurately characterizes the operation environment is the key to obtaining an effective threshold value. As an

\*Y. A. Şekercioğlu is with Monash University, Department of Electrical and Computer Systems Engineering, Clayton, Victoria, Australia

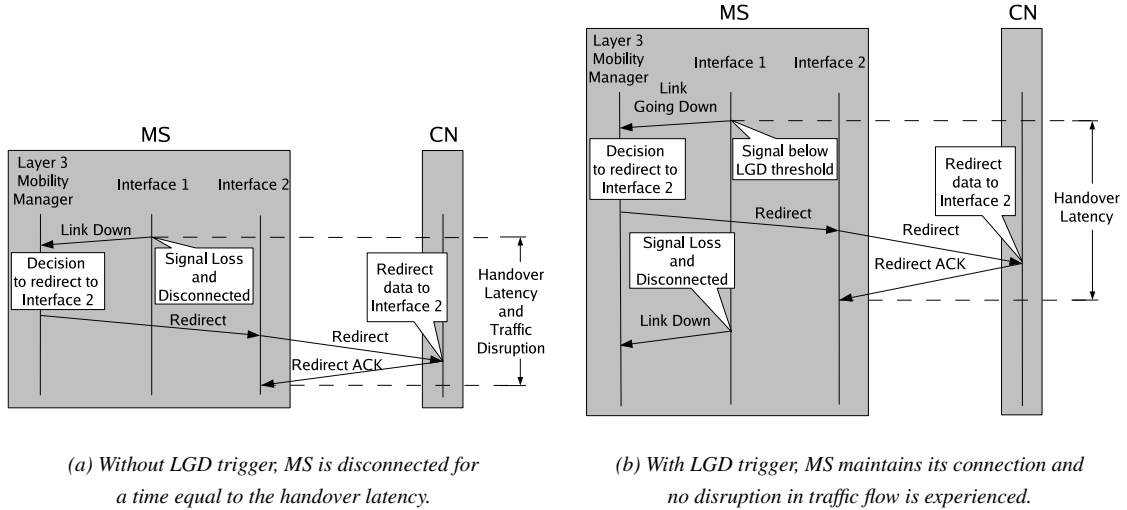


Figure 1: Multiple interface handover with Triggers

example, let's assume the Fritz path loss model [10] shown in (2):

$$\left[ \frac{P_{rx}(d)}{P_{rx}(d_0)} \right]_{dB} = -10\beta \log \left( \frac{d}{d_0} \right) \quad (2)$$

where  $P_{rx}$  is the received signal power level in Watts,  $\beta$  is the path loss exponent, and  $d$  is the distance between the receiver and the transmitter expressed in meters. Also note that  $P_{rx}(d_0)$  is the received power at the close-in reference distance,  $d_0$ , and can be determined using the free space path loss model.

The MS monitors its received signal strength through data sent from the Access Point (AP). Hence, in the context of these equations, the MS and AP are the receiver and transmitter respectively. Assuming the MS starts at the AP and moves at a constant velocity  $v$  radially from the AP at time  $t$  equal to zero,  $R_{time}$  can be determined as:

$$R_{time} = 1 - \frac{d_0}{vt_{new}} \left( \frac{P_{rx}(d_0)}{P_{rxthresh}} \right)^{\frac{1}{\beta}} \left[ 1 - \frac{1}{\alpha^{\frac{1}{\beta}}} \right] \quad (3)$$

where  $t_{new}$  is the time to establish the new interface connection.

Thus, knowing  $v$ ,  $t_{new}$ , and  $P_{lgd}$  of the MS, (3) allows one to estimate the ratio of packets lost during a handover,  $R_{packet}$ . This calculation assumes traffic sent at a constant rate. In section IV a numerical fitting method is presented and evaluated in order to address the case for bursty traffic.

#### IV. PERFORMANCE RESULTS

In this section we evaluate the model described previously for effectively setting the LGD trigger threshold. We start by describing the simulation configuration, and present results under ideal path loss conditions. Following this, we show how the model can be extended to address shadowing effects and bursty traffic.

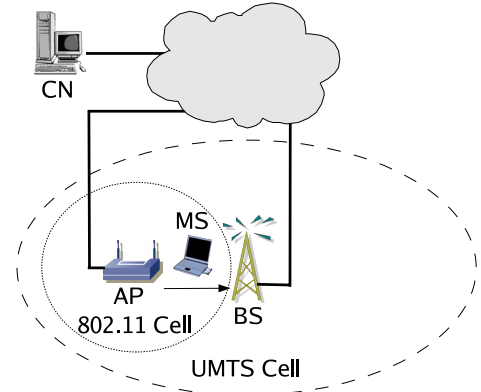


Figure 2: Simulation scenario

##### A. Simulation configuration

The scenario illustrated in Fig. 2 was simulated using the ns-2 [9] simulator to verify and evaluate the model discussed previously. In particular, the simulation results were used in order to identify suitable parameter values for setting the LGD threshold.

The scenario consists of an IEEE 802.11 cell, overlapped with a UMTS cell offering a wider coverage area. Initially the MS will start within the WLAN cell 2 meters away from the WLAN AP. It then detects the AP (through active or passive scanning) and performs the association handshake process. Once this is completed, the Correspondent Node (CN) starts sending a Constant Bit Rate (CBR) traffic stream with a packet size of 604 bytes (including UDP, IP, and MAC header) at 0.02 second intervals. The MS begins moving away from the AP at a constant speed while receiving packets from the CN. Eventually, it reaches a point where the signal level is below  $P_{rxthresh}$  and it needs to perform a handover to the UMTS cell. By triggering an LGD event when the signal level reaches  $P_{lgd}$ , assuming sufficient anticipation is provided, the number of pack-

Path Loss Model Configuration	
Transmit Power ( $P_t$ )	0.025W
Wavelength ( $\lambda$ )	0.124m
Path Loss Exponent ( $\beta$ )	4
Standard Deviation ( $\sigma$ )	0dB to 4dB
Receive Power ( $P_{rx}$ )	$3.162 \times 10^{-11}W$

Table 1: Simulation Parameters

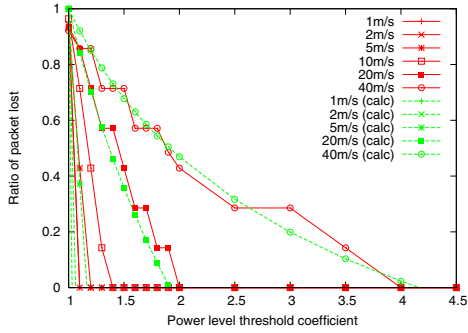


Figure 3:  $R_{packet}$  during handover with  $\sigma = 0$  and  $\delta = 1$

ets lost during a handover is minimized. In this scenario, it is assumed that the UMTS interface on the MS already knows which BS to connect to. Therefore, only a layer 3 handover is required when switching to the new interface. The MS then updates the CN to redirect the traffic flow to its new interface.

### B. Validation of the Handover Loss Equation

It can be seen from Fig. 3 that the  $R_{packet}$  expected, obtained by using (3) corresponds well to the one obtained by simulation. MSs with a speed of 10 m/s and under move slowly enough that the binding update can be completed without any loss with a  $P_{lgd}$  less than 1.5 times  $P_{rx}$ . More significant anticipation is required at higher speeds that exceed 20 m/s.

### C. Effects of Shadowing

After studying the packet lost during a handover for an ideal decaying signal, we will now investigate shadowing effects which may affect the propagation model. These shadowing effects can be modeled by introducing an additional component  $X_\sigma$ , to the Fritz path loss model shown in (2).

$$\left[ \frac{P_{rx}(d)}{P_{rx}(d_0)} \right]_{dB} = -10\beta \log \left( \frac{d}{d_0} \right) + X_\sigma \quad (4)$$

$X_\sigma$  is a random variable drawn from a Gaussian distribution with a standard deviation of  $\sigma$  [10]. Note that, a 0 value for  $\sigma$  indicates the absence of any shadowing effects.

Comparing the simulation results presented in Fig. 3, Fig. 4, and Fig. 5 indicates that, increasing shadowing effects (represented by higher  $\sigma$  values) require larger  $P_{lgd}$  to constrain the packet losses during a handover. This is due to the higher signal variation increasing the probability of receiving a packet below  $P_{rxthresh}$ , as the MS moves away from the AP. Hence,  $P_{lgd}$  needs to be set higher to compensate. Notice also, from

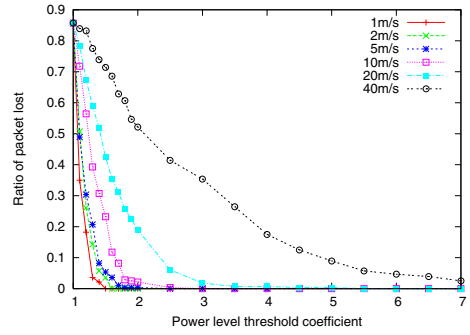


Figure 4:  $R_{packet}$  during handover with  $\sigma = 1$  and  $\delta = 1$

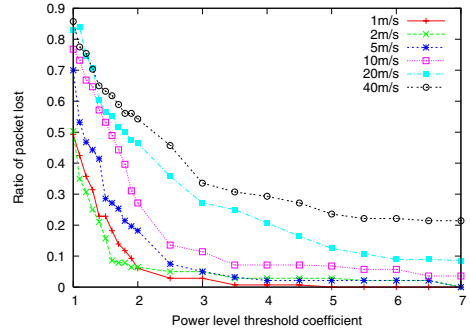


Figure 5:  $R_{packet}$  during handover with  $\sigma = 4$  and  $\delta = 1$

Fig. 5 that slower MSs have a packet loss lower than expected for  $P_{lgd}$  close to  $P_{rxthresh}$ . This is due to the signal level of packets occasionally reaching above  $P_{rxthresh}$ . Only slower MSs which spends more time at this border, experience this phenomenon. It is clear that results from (3) do not apply when shadowing is introduced.

A relationship between the  $\alpha$  values of two MS with different velocities, but the same  $R_{time}$  can be derived, as seen in (5). This can then be used to interpolate the  $R_{time}$  for MSs at different speeds, when measurements for one speed is known. The results shown in Fig. 6 demonstrate the interpolated curves (marked by dotted lines), when measurements for a 10 m/s MS were used as reference points. Although not perfect, these interpolated estimates provide better accuracy than (3) in approximating  $R_{packet}$ .

$$\alpha_2 = \frac{1}{\left[ 1 + \frac{v_2}{v_1} \left( \frac{1 - \alpha_1^{\frac{1}{\beta}}}{\alpha_1^{\frac{1}{\beta}}} \right) \right]^\beta} \quad (5)$$

### D. Weighted Averaging of Signal Strength

By introducing the shadowing effects to achieve a more realistic path loss model, it is important to include a weighted averaging mechanism to produce a stable signal strength reading. It is particularly important when the shadowing component becomes significant. To achieve this, a simple weighted average (seen in (6)) is maintained. Note that a  $\delta$  equal to one, is the

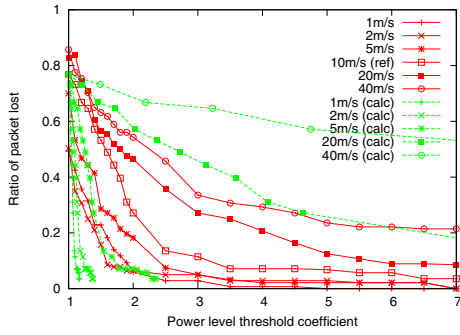


Figure 6:  $R_{packet}$  during handover with  $\sigma = 4$ ,  $\delta = 1$ , and interpolation based on 10 m/s MS.

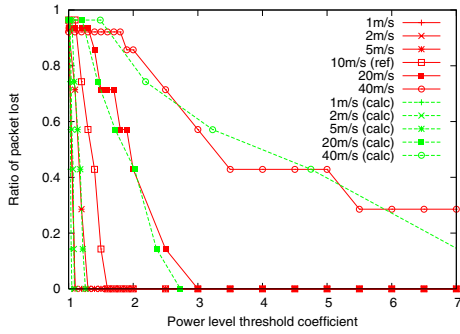


Figure 7:  $R_{packet}$  during handover with  $\sigma = 0$ ,  $\delta = 0.25$ , and interpolation based on 10 m/s MS.

same as using an instantaneous reading with no averaging applied.

$$P_{avg} = \delta P_{new\_reading} + (1 - \delta) P_{old\_avg} \quad (6)$$

First, we apply the weighted averaging to signal strength samples without shadowing ( $\sigma = 0$ ) in order to investigate the effects of averaging independent of shadowing. Comparing Fig. 7 to Fig. 3, it can be seen that as more averaging is applied (lower  $\delta$ ) the system becomes less responsive to rapid changes. Hence, a higher  $\alpha$  value is required in order to achieve the same level of anticipation and the same ratio of packet lost. From this, it is clear that (3) does not apply when averaging is used. However, it can be seen in Fig. 7 that it is possible to use (5) to approximate the curves reasonably accurately, as long as one curve for a given speed is known. The plots obtained through simulations seem to correspond well with the interpolated plots. As for the previous section, the measurements for a MS moving at 10 m/s were used as a reference points to produce the interpolated curves.

An appropriate value for  $\delta$  will largely depend on the amount of signal variation (i.e., value of  $\sigma$ ), and it is currently chosen experimentally. Other techniques may be applied, however, this is left as part of the future work. Fig. 8 shows the possible signal strength variations for different  $\delta$  values, when  $\sigma$  is set to 4. The variation swing can be seen to be quite large without any averaging applied, while 0.25 or 0.05 stabilizes the readings quite acceptably. It is important to obtain stabil-

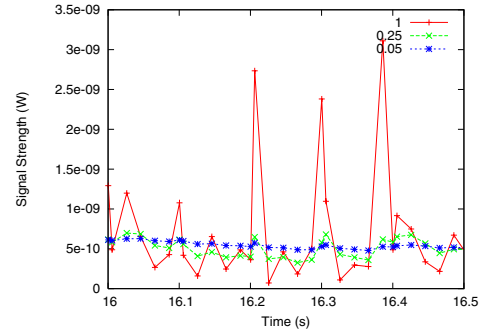


Figure 8: Average signal strength (for  $\delta$  values of 0.05, 0.25 and 1) as the MS moves away from the AP.

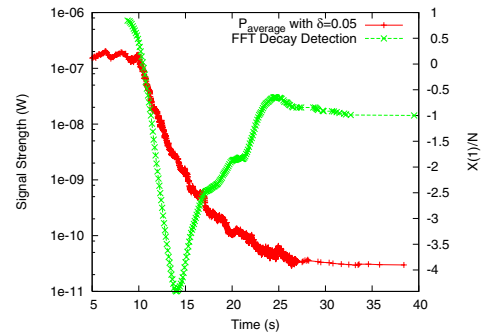


Figure 9: Average signal strength and FFT decay detection value as the MS moves away from the AP with  $\delta = 0.05$

ity to reduce the likelihood of a ping pong effect, in our case oscillating between Link Going Down and Link Rollback.

Next we compare the decaying signal produced using a  $\delta$  of 0.05 to the Fast Fourier Transform (FFT) based decay detection method described in [4]. We use a sampling interval of 100 ms, and an FFT threshold  $X(1)/N$  equal to -0.6, which means the signal is considered to be decaying when the FFT method is below this value. Fig. 9 demonstrates that both the weighted averaging and FFT-based decay detection method lead to comparable results. As suggested by the authors of [4], both methods may be used in combination to determine a decaying signal.

The amount of averaging applied should be chosen to adequately stabilize the signal strength samples. However, as more averaging is applied, further anticipation is required to compensate the slower response, by increasing the value of  $\alpha$ .

It can be seen in Fig. 10 that when the weighted averaging is applied to a shadowing signal, the consistency of handover loss seems to improve, resulting in better interpolated curves. However, it is still only good enough to be used as a rough guide for estimating appropriate thresholds, especially for fast moving MSs.

#### E. Video traffic patterns

In the previous section, we developed a method based on interpolation to estimate appropriate thresholds. Now we will see how well this technique can be applied to bursty traffic, similar to video traffic streams. The traffic pattern is quite different

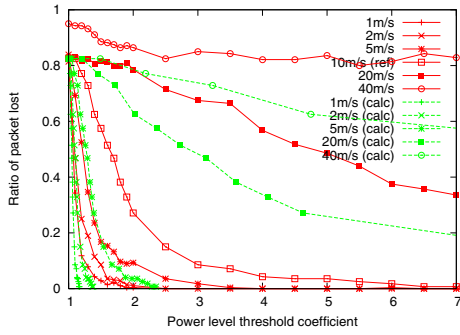


Figure 10:  $R_{packet}$  during handover with  $\sigma = 4$ ,  $\delta = 0.05$ , and interpolation based on 10 m/s MS.

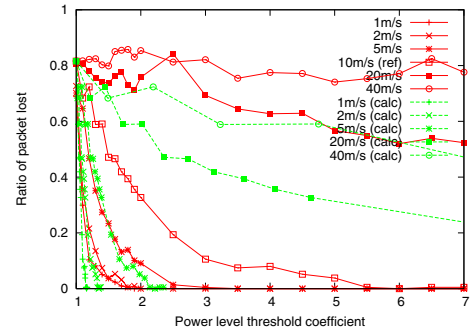


Figure 12:  $R_{packet}$  during handover for Video traffic with  $\sigma = 4$ ,  $\delta = 0.05$ , and interpolation based on 10 m/s MS.

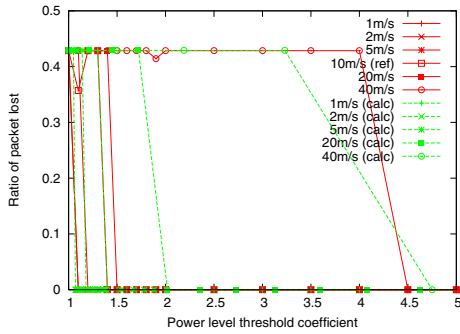


Figure 11:  $R_{packet}$  during handover for Video traffic with  $\sigma = 0$ ,  $\delta = 1$ , and interpolation based on 10 m/s MS.

compared to CBR traffic. Generally it sends a burst of a few packets at intervals, rather than one packet at a time at fixed intervals. To simulate bursty video traffic, a burst of three 1000 byte packets are sent at 0.07 second intervals. This equates to a rate of 0.023 seconds per packet, which will be used to calculate the expected packets during the handover period with (3).

Since the number of send attempts during the handover period and weighted averaging update process depends on the traffic pattern, a different  $R_{packet}$  trend will result compared to the case using CBR traffic. This can be seen by comparing Fig. 11 with Fig. 3, and Fig. 12 with Fig. 10. As for the case of using CBR traffic, a sufficient  $\delta$  need to be chosen to handle the amount of shadowing. Interpolation estimates, as done for CBR traffic with shadowing and weighted averaging, can be used for bursty traffic as well. Estimates for both traffic types exhibit a similar behavior and decreases in accuracy for MS with higher speeds.

## V. CONCLUSION

In this paper, the handover performance of a MS equipped with multiple interfaces switching from one interface to another was investigated. By using link triggers, specifically the LGD trigger based on signal strength readings, the MS was able to establish a new connection on another interface, before the current interface disconnects. An equation based on the Fritz path loss model was developed to relate the ratio of packet lost during handover to the threshold coefficient  $\alpha$ . This equation helps

determine a suitable  $\alpha$  value to provide sufficient anticipation to minimize handover packet loss for MSs moving at different speeds. In order to address realistic scenarios where the signal level fluctuates due to shadowing effects or bursty traffic, additional methods including averaging and interpolation were presented and evaluated. In particular, a numerical method was developed to interpolate the threshold coefficient relationships at various MS speeds, given some knowledge of the signal decay patterns for a specific speed. It was shown that this can be used effectively in order to set the LGD threshold.

## REFERENCES

- [1] IEEE 802.21 Task Group, <http://www.ieee802.org/21/>.
- [2] B. Aboda. Architectural Implications of Link Indications, Internet Engineering Task Force Internet Draft, draft-iab-link-indications-04.txt, December 2005.
- [3] K. Chebrolu and R. Rao. Communication Using Multiple Wireless Interfaces. In *Proceedings of the IEEE Wireless Communications and Networking Conference WCNC'02*, pages 327–331, Florida, United States of America, March 2002.
- [4] C. Guo, Z. Guo, Q. Zhang, and W. Zhu. A Seamless and Proactive End-to-End Mobility Solution for Roaming Across Heterogeneous Wireless Networks. *IEEE Journal on Selected Areas in Communications*, 22(5):834–848, June 2004.
- [5] E. Gustafsson and A. Jonsson. Always Best Connected. *IEEE Wireless Communications*, 10(1):49–55, February 2003.
- [6] A. Mishra, M. Shin, and W. Arbaugh. An Empirical Analysis of the IEEE 802.11 MAC Layer Handoff Process. *ACM SIGCOMM Computer Communication Review*, 33(2):93–102, 2003.
- [7] N. Montavont, E. Njedjou, F. Lebeugle, and T. Noel. Link Triggers Assisted Optimizations for Mobile IPv4/v6 Vertical Handovers. In *Proceedings of the IEEE Symposium on Computers and Communications ISCC'05*, pages 289–294, Cartagena, Spain, June 2005.
- [8] N. Montavont and T. Noel. Handover Management for Mobile Nodes in IPv6 Networks. *IEEE Communications Magazine*, 40(8):38–43, August 2002.
- [9] The Network Simulator - ns-2. URL reference: <http://www.isi.edu/nsnam/ns/>.
- [10] Theodore S. Rappaport. *Wireless Communications: Principles and Practice*. Pearson Education International, 2002.
- [11] G. Wu, M. Mizuno, and P. Havinga. MIRAI Architecture for Heterogeneous Network. *IEEE Communications Magazine*, 40(2):126–134, February 2002.